

Operation of Joule-Thomson Refrigeration Above the Critical Pressure of Helium

D. L. Johnson

Radio Frequency and Microwave Subsystems Section

Recent emphasis on energy conservation has resulted in new efforts to develop more efficient, long-life refrigeration techniques for the DSN maser. As the new techniques are developed, a comparison of their reliability and efficiency to those of the closed-cycle helium refrigerator presently used will have to be made. Measurements of the refrigeration capacity have been made on an existing refrigeration system as a function of the supply pressure and the return pressure in the Joule-Thomson circuit. The performance of the refrigerator has been calculated and compared to the ideal Carnot-cycle refrigerator.

I. Introduction

A new effort has been undertaken to study efficient, long-life refrigeration techniques for the DSN masers. Key areas requiring study and development are (1) highly efficient helium compression techniques capable of long unattended operation, (2) long-life seals and bearings, (3) improved system integration to increase the efficiency in the Joule-Thomson cooling process or (4) finding alternatives to the Joule-Thomson process, such as adiabatic demagnetization, to provide liquid helium temperatures at increased efficiencies.

The closed-cycle helium refrigerators (CCRs) currently in use in the DSN were developed long before energy conservation became a major concern such that reliability was achieved at the expense of efficiency. As a result over one million hours of operation has been logged on some thirty CCRs that have been installed in the DSN since 1967 (Ref. 1). However, the CCR operates between room temperature and liquid helium temperatures with only about one percent of Carnot efficiency in producing one watt of refrigeration at 4.5 K.

As possible steps to improve upon the efficiency of the CCR, studies and development are presently being undertaken in each of the three basic subsystems of the CCR: the compressor unit; the expansion engine, which provides refrigeration down to 15 K; and the Joule-Thomson (J-T) circuit, which provides the final refrigeration between 15 and 4.5 K. A schematic diagram of the CCR is shown in Fig. 1.

In an effort to reduce the electrical input power required to operate the compressor system, a new concept in the mechanical compression of a gas has been under development. In the new approach, a centrifugal-reciprocating compressor concept has been developed which utilizes the centrifugal forces produced by the rotating pistons and the housing assembly to assist in the compression of the helium gas. The performance of a single stage feasibility model has been demonstrated, and a mathematical analysis of the machine has been published (Ref. 2). A patent application has been filed by NASA for the centrifugal-reciprocating compressor.

In another area of development the regenerator matrix materials used in the 15 K expansion engine of the CCR are being studied. The 15 K expansion engine utilizes the Gifford-McMahon thermodynamic cycle and has proven very reliable. It is expected that the efficiency and reliability of the expansion engine may be improved by either improving upon the matrix of the presently used regenerator material or by using a substitute material. Lake Shore Cryotronics, Inc., under contract to JPL (Ref. 3), has developed a ceramic material which is thermodynamically superior (for $T < 25$ K) to the lead shot presently used as a regenerator material. Testing of this ceramic material in an expansion engine will soon be conducted to measure its performance.

Adiabatic demagnetization refrigeration (magnetic cooling) is yet another area of study and development. The magnetic cooling process is being studied as a possible replacement of the J-T circuit now used in the CCR to provide the final stage of refrigeration. Two major advantages of the magnetic cooling process over the J-T process would be its high reliability (since it is a solid state technique) and its high efficiency (60-80 percent of Carnot efficiency between 4.5 K and 15 K, compared with approximately 20 percent of Carnot efficiency for the J-T expansion circuit over the same temperature range). After initial testing of the paramagnetic salts, an experimental magnetic cooling system will be built and tested.

The three areas of study and development mentioned above will be the subject of individual reports to be presented at a later time and thus will not be discussed further in this report. Rather, the scope of this report has been focused on the operation of the present CCR to determine its refrigeration capacity under various operating conditions. It is felt that the study of a more efficient refrigeration system should begin with a complete understanding of the refrigeration system as it presently exists. This then provides the baseline for a comparative study as new materials or methods of operation are integrated into the system.

The refrigeration capacity for the present CCR was measured in two separate tests. First, the capacity was determined for various J-T supply pressures and various refrigerator supply pressures while holding a constant J-T return pressure. Second, the capacity was again measured, this time as a function of the J-T return pressure while maintaining constant supply pressures to both the J-T circuit and the expansion engine. In the second test particular attention was paid to the capacity measurements for return pressures above the critical pressure of helium (2.27×10^5 N/m² (33 psia)) to determine how well the Joule-Thomson circuit would regulate when no liquid was being produced. The performance of the CCR under these conditions was then calculated and compared to the ideal Carnot-cycle refrigerator. Before discussing these tests

and the test results, the method of thermometry used will first be described.

II. Temperature Monitors

Temperature determination at the 4.5 K station was handled by two methods: resistance thermometry and vapor pressure/gas thermometry. A Lake Shore Cryotronics digital thermometer (Model DRC-70C) provided direct temperature readings using a silicon diode (Model DT-500-Cu) placed at the 4.5 K station (see Fig. 1). A vapor pressure transducer, located in close proximity to the diode, connects to a pressure gauge outside the refrigerator and provides the other means of temperature sensing. The temperature of this station dictates the pressure of the gas within the gauge. At very low temperatures, a portion of the gas within the transducer will liquify. In the small range of temperatures for which this liquid and its vapor will exist in equilibrium, the pressure gauge readings may be compared to a known temperature-vapor pressure curve to determine the temperature at the cold station. Above this temperature range the device behaves as a gas thermometer, with the pressure readings being proportional to the temperature.

The relationship between the two temperature sensing devices at various temperatures was measured by adjusting the J-T return pressure and by applying resistive heating to the 4.5 K station. The results are shown in Fig. 2 with the resistance thermometer readings plotted on the y-axis and vapor pressure readings plotted along the x-axis. Also shown is the curve for the accepted values for the temperature-vapor pressure relationship as tabulated in the *American Institute of Physics Handbook* (Ref. 4). The 0.1 K difference between the curves at the low pressures may be attributable to the calibration error of the digital thermometer. The measured data were not corrected for this error. The diode has been temperature cycled several times and has shown good repeatability in the data. The 0.1 K sensitivity limit of the digital readout adds some additional uncertainty to the data at the low pressures. The vapor pressure device was unable to maintain a liquid/vapor equilibrium to the 2.27×10^5 N/m² (5.2 K) limit as shown by the deviation of the shape of the measured curve from the AIP curve near 1.86×10^5 N/m² (27 psia). Thus, the vapor pressure thermometer should not be relied upon for accurate temperature measurements above 1.86×10^5 N/m² (4.9 K) where the device changes to a gas thermometer.

III. Refrigeration Capacity Measurements

For a fixed pressure operation, the refrigeration capacity at the 4.5 K station of the CCR is determined primarily by the flow rate in the J-T circuit, by the temperature of the

15 K station, and by the efficiency of the heat exchanger between the 15 K station and the J-T valve. This capacity is equal to the heat of vaporization of the liquid helium produced by the J-T expansion plus the heat capacity of the cooled gas that had not liquified by the J-T expansion. Electrical input power levels below the cooling capacity will vaporize a fraction of the liquid reserve before reaching a new liquid/vapor equilibrium; power levels in excess of this cooling capacity will deplete the liquid reserve and warm the refrigerator. It has also been observed that above 5.2 K, the critical temperature at which liquid helium can be maintained, the cooled gas from the expansion process also has a significant cooling capacity. This will be discussed shortly.

Determination of the refrigeration capacity of the CCR was made by applying an electrical load to the resistive heating element located on the 4.5 K station. An electrical power load above the assumed capacity was applied to quickly deplete the reserve liquid in the system, causing the temperature and vapor pressure at this station to rise. By incrementally decreasing the input power, the temperature and the vapor pressure were kept from rising above a nominal 4.8 K and 1.72×10^5 N/m² (25 psia), respectively (well below the critical temperature and pressure of 5.2 K and 2.27×10^5 N/m² (33 psia), respectively), so that the J-T expansion process would continue to produce liquid. When the power was decreased to below the cooling capacity, the temperature and the vapor pressure dropped, indicating liquid was being stored. This provided a quick method of approximating the capacity. A more accurate capacity determination could then be made by applying power levels about this point for periods as long as one hour to determine the highest input power for which the temperature and the vapor pressure would stabilize. In this manner the refrigeration capacity has been measured for three J-T supply pressures and two different refrigerator supply pressures while holding the J-T return pressure constant. The results are tabulated in Table 1, where the refrigeration capacity has been denoted as Q_{meas} and the temperature of 4.5 K station as T_C . (The remainder of the data in the table will be discussed later.) The capacity measurements were made throughout the day, during which the ambient temperature surrounding the compressors would change. The effect of the daily temperature cycling has been observed to produce up to a 50-mW capacity change on previous CCRs. However, temperature changes of 7°C during the measurements on this CCR showed no noticeable change in the refrigeration capacity.

The temperature variation as a function of the J-T return pressure and the various heat loads was also monitored. The results have been tabulated in Table 2 and are shown in Figs. 3 and 4. In Fig. 3 the temperature at the 4.5 K station has been plotted as a function of the applied heat loads. The values for the constant pressure curves are given for the no

load condition since at the higher heater power levels the return pressure will decrease slightly. Each pressure curve ends at the highest heater power for which the temperatures and pressures would stabilize; increasing the heater power beyond this point would cause the refrigerator to warm excessively. (The power levels could be incremented in approximately 20-mW intervals.) The maximum power level at which the stabilization occurs may be considered the cooling capacity for that particular J-T return pressure (or for that particular temperature).

Figure 3 shows that there is a nearly linear degradation in cooling capacity as the temperature is increased from 4.5 to 8 K, and that there is still a significant cooling capacity for temperatures above 5.2 K, the critical temperature above which liquid helium cannot exist. Above this critical temperature the refrigeration capacity must be obtained non-isothermally from the sensible heat of the gas rather than from the isothermal heat of vaporization. Although temperature and pressure regulation at the 4.5 K station should be difficult to maintain because of the low thermal capacity of the helium gas, the data show very little temperature change with change in heater power for temperatures below 6 K.

While the present CCR relies on the liquid helium reserve to insure additional temperature stability, the operation of the CCR at increased J-T return pressures (so that the cold station temperature is above 5.2 K) also provides reasonable temperature stability. This depends on the provision that the heat load of the device being cooled is sufficiently less than the refrigeration capacity of the CCR under these operating conditions.

For the CCR tested, operating the J-T return pressure as high as 3.10×10^5 N/m² (3 atm) increased the temperature by only 1.1 K over the nominal 4.5 K achieved for the normal operating return pressure of just over an atmosphere. This result is significant as there are numerous applications (such as cooling superconducting magnets or Josephson devices) that could be satisfied with an efficient and reliable 5.5 K refrigerator. Another application could be the cooling of a maser since the refrigeration capacity of the CCR at 5.5 K is much greater than the heatload produced by an operating maser. Although it may be desirable to optimize maser performance by operating the maser as cold as possible (Ref. 5), there are other factors, such as energy requirements and reliability, which determine the necessary trade-offs to establish the temperature that provides the best overall performance. The higher return pressure would permit a reduction in the electrical power requirements by operating with smaller compressors, which may also have the added advantages of prolonged maintenance-free operating times and an increased overall lifetime of the system.

Figure 4 shows the temperature at the 4.5 K station as a function of the J-T return pressure. Portions of several constant power curves have also been shown. The vapor pressure curve has also been placed on the graph to show the similar shape between the vapor pressure curve and the J-T return pressure when no heater power is applied. The return pressure curve appears to be a direct extension of the vapor pressure curve showing no discontinuity or change in slope as it extends beyond $2.27 \times 10^5 \text{ N/m}^2$ (33 psia). The pressure differences between the two curves occur because the J-T return pressure gauge monitors the pressure at the room temperature gas line rather than at the 4.5 K station. Restriction in the heat exchanger causes the pressure at the external pressure gauge to be lower than indicated by the vapor pressure gauge. (It should be noted that the pressure drop due to this restriction has a small effect on the available refrigeration capacity and directly affects the temperature at which the refrigeration takes place (Ref. 6).) The appropriate test points for pressure and temperature measurements are shown in Fig. 1.

IV. Refrigerator Performance Analysis

When a heat load corresponding to the cooling capacity of the machine is applied at the 4.5 K station, the temperatures of the incoming and outgoing streams of gas just above the third exchanger are equal. Were they not, the system would either cool down or warm up. To determine the performance of the J-T loop below the 15 K station, the remainder of the refrigerator may be thought of as a single compressor operating at 15 K. This refrigerator may then be analyzed as if it were a Linde-Hampson refrigerator as shown in Fig. 5. The Linde-Hampson refrigerator has been discussed thoroughly elsewhere (e.g., see Refs. 7, 8, and 9) so only a brief review of the analysis will be presented here.

It will be assumed that the final heat exchanger is 100 percent effective, that there are no heat leaks into or out of the system, and that the J-T expansion represents the only irreversible pressure drop throughout the cycle shown in Fig. 5. Under these conditions the heat absorbed from the source during one complete cycle may be expressed as

$$\frac{Q_{\text{ref}}}{\dot{m}} = h_1 - h_2$$

that is, the net refrigeration per unit flow rate depends solely on the enthalpies of the incoming and outgoing gases, and is independent of what happens below the top of the heat exchanger. If liquid is produced, the net work required by the

compressor during one cycle (1-2-3-4-1) is

$$\frac{W_{\text{net}}}{\dot{m}} = T_H (S_1 - S_2) - x(h_g - h_f) + (h_2 - h_3) - (h_1 - h_g)$$

where

$$x = (h_1 - h_2) / (h_1 - h_f)$$

is the fraction of the gas liquified and

$$h_3 = xh_f + (1 - x)h_g$$

If no liquid is produced, the cycle follows path (1-2-3'-4'-1), and the net work required is

$$\frac{W_{\text{net}}}{\dot{m}} = T_H (S_1 - S_2) - (h_1 - h_2)$$

The performance of the refrigerator is expressed as the coefficient of performance by

$$COP = \frac{Q_{\text{ref}}}{W_{\text{net}}}$$

The efficiency of this refrigerator is determined by using the figure of merit of the refrigerator, defined by

$$FOM = \frac{COP}{COP_c} = \frac{Q_{\text{ref}}/W_{\text{net}}}{T_C/(T_H - T_C)}$$

where COP_c is the coefficient of performance for a reversible Carnot cycle, and the FOM varies from zero to unity. The coefficient of performance and the figure of merit for the measured refrigeration capacity may be evaluated in the same manner.

The results for the analysis have been included in Tables 1 and 2. The values for the entropies and the enthalpies used to determine W_{net} and Q_{ref} were estimated from the temperature-entropy diagram given in Ref. 10. As the only other non-measured parameter, T_H was assumed to remain constant at 15 K throughout the measurements since there was no provision made to measure the temperature of the 15 K station. The 15 K temperature is representative of the temperature of the 15 K station of the CCR when cooling a maser amplifier. Heat loads in excess of this amount would raise the temperature of this station by an unknown additional

amount, resulting in a smaller difference between Q_{meas} and Q_{ref} (which depends on this temperature).

The results shown in Table 1 indicate that operating at the higher refrigerator supply pressure increased the refrigeration capacity at the 4.5 K station. The increased supply pressure results in a lower temperature at the 15 K station. In turn, the temperature of the J-T supply gas, which is in a recuperative heat exchange with the 15 K station, is lowered. Expanding the gas at the lower temperature results in the increased cooling capacity. The data presented in Table 2 show that the capacity increases with decreasing return pressure. This is also consistent with the temperature-entropy diagram. However, to insure contaminants will not be drawn into the gas lines, a positive pressure is maintained for the J-T return gas.

V. Summary

Several important facts have been established with the testing of this CCR, which may be considered representative

of all DSN CCRs. First, the vapor pressure gauge worked very well at the extreme low temperatures, but should not be relied upon beyond $1.86 \times 10^5 \text{ N/m}^2$ (27 psia) (4.9 K), where it prematurely begins to function as a gas thermometer. In contrast, the resistance thermometer showed a very small but constant error across the 4 through 8 K range, which could be corrected to give accurate temperature readings. Second, the maximum cooling capacity of this particular CCR was determined to be 1.00 W when operating with a refrigerator supply pressure of $2.20 \times 10^6 \text{ N/m}^2$ (305 psig), a J-T supply pressure and return pressure of $1.82 \times 10^6 \text{ N/m}^2$ (250 psig) and $1.11 \times 10^5 \text{ N/m}^2$ (16.1 psia), respectively, and a compressor temperature of 25°C. Finally, the refrigeration capacity and the temperature stability for J-T regulation above the critical temperature and pressure of 5.2 K and $2.27 \times 10^5 \text{ N/m}^2$ (33 psia) remained quite high for temperatures and return pressures as high as 6 K and $3.44 \times 10^5 \text{ N/m}^2$ (50 psia), respectively. This cooling capacity at the increased return pressures is significant and may permit the utilization of smaller compressors with reduced power requirements.

References

1. Higa, W. H., and Wiebe E., "One Million Hours at 4.5 Kelvin," *Proc. App. of Closed-Cycle Cryocoolers to Small Superconducting Devices*, pp. 99-108, Boulder, Colorado, Oct. 1978 (published as NBS Spec. Pub. 508).
2. Higa, W. H., *On the Characteristics of Centrifugal-Reciprocating Machines*, JPL Publication 79-108, Jet Propulsion Laboratory, Pasadena, California, Dec. 1979.
3. JPL Contract No. 955446 entered with Lake Shore Cryotronics Inc., and the Jet Propulsion Laboratory.
4. *American Institute of Physics Handbook*, Second Edition, edited by D. E. Gray, McGraw-Hill Book Company, Inc., New York, 1963.
5. Siegman, A. E., *Microwave Solid-State Masers*, Chapter 7, McGraw-Hill Book Company, New York, 1964.
6. Dean, J. W., and Mann, D. B., "The Joule-Thomson Process in Cryogenic Refrigeration Systems," NBS Technical Note 227, National Bureau of Standards, Boulder, Colorado, 1965.
7. Daunt, J. G., "The Production of Low Temperatures Down to Liquid Hydrogen," in *Encyclopedia of Physics, Vol. XIV: Low Temperature Physics I*, edited by S. Flügge, Springer-Verlag, Berlin, Göttingen, Heidelberg, 1956.
8. Scott, R. B., *Cryogenic Engineering*, D. Van Nostrand Company, Inc., Princeton, 1959.
9. Barron, R., *Cryogenic Systems*, McGraw-Hill Book Company, New York, 1966.
10. McCarty, R. D., "Thermodynamic Properties of Helium 4 from 2 to 1500 K at Pressures to 10^8 Pa ," *J. Phys. Chem. Ref. Data*, Vol. 2, p. 923, 1973.

Table 1. Refrigeration capacity as a function of refrigerator supply pressure and J-T supply pressure

Refrigerator Supply, $\text{N/m}^2 \times 10^5$ (psig)	22.04 (305)	22.04 (305)	22.04 (305)	20.31 (280)	20.31 (280)
Refrigerator Return, $\text{N/m}^2 \times 10^5$ (psig)	8.60 (110)	8.60 (110)	8.60 (110)	7.91 (100)	7.91 (100)
J-T Supply, $\text{N/m}^2 \times 10^5$ (psig)	20.31 (280)	18.25 (250)	16.18 (220)	18.25 (250)	16.18 (220)
J-T Return, $\text{N/m}^2 \times 10^5$ (psia)	1.11 (16.1)	1.11 (16.1)	1.11 (16.1)	1.11 (16.1)	1.11 (16.1)
J-T Flow, SCFM	1.48	1.39	1.25	1.38	1.28
T_C , K	4.7	4.6	4.5	4.5	4.5
COP_c	0.456	0.442	0.429	0.429	0.429
W_{net} , W	10.82	9.87	8.61	9.79	8.85
Q_{meas} , W (± 0.02 W)	1.037	1.000	0.834	0.896	0.795
COP_{meas}	0.0958	0.101	0.0969	0.0915	0.0898
FOM_{meas}	0.210	0.229	0.226	0.213	0.209
Q_{ref}	1.81	1.60	1.31	1.59	1.35
COP_{ref}	0.168	0.162	0.152	0.162	0.153
FOM_{ref}	0.368	0.367	0.354	0.378	0.357
$T_H = 15$ K					
CCR tested: SN 78005					

Table 2. Refrigeration capacity as a function of J-T return pressure

$P_1, \text{N/m}^2 \times 10^5 \text{ (atm)}$	1.11 (1.1)	1.82 (1.8)	2.33 (2.3)	2.74 (2.7)	3.24 (3.2)	3.95 (3.9)	4.96 (4.9)	5.98 (5.9)
J-T Flow, SCFM	1.39	1.22	1.20	1.17	1.13	1.05	0.99	0.90
T_C, K	4.6	5.2	5.7	6.0	6.5	7.3	8.1	8.6
COP_c	0.442	0.531	0.613	0.667	0.765	0.948	1.17	1.34
W_{net}, W	9.87	7.11	6.32	5.45	4.81	4.15	3.34	2.58
$Q_{\text{meas}}, \text{W} (\pm 0.02 \text{ W})$	1.000	0.896	0.803	0.703	0.616	0.489	0.396	0.294
COP_{meas}	0.101	0.126	0.127	0.129	0.128	0.118	0.119	0.114
FOM_{meas}	0.229	0.237	0.207	0.193	0.167	0.124	0.101	0.0851
Q_{ref}, W	1.60	1.31	1.21	1.13	1.05	0.884	0.726	0.606
COP_{ref}	0.162	0.184	0.191	0.207	0.218	0.213	0.217	0.235
FOM_{ref}	0.367	0.347	0.312	0.310	0.285	0.225	0.185	0.175
Refrigerator supply: $22.04 \times 10^5 \text{ N/m}^2$ (305 psig)				J-T Supply: $18.25 \times 10^5 \text{ N/m}^2$ (250 psig)				
Refrigerator return: $8.60 \times 10^5 \text{ N/m}^2$ (110 psig)				$T_H = 15 \text{ K}$				
$P_2 = 18.25 \times 10^5 \text{ N/m}^2$ (18 atm)				CCR tested: SN 78005				

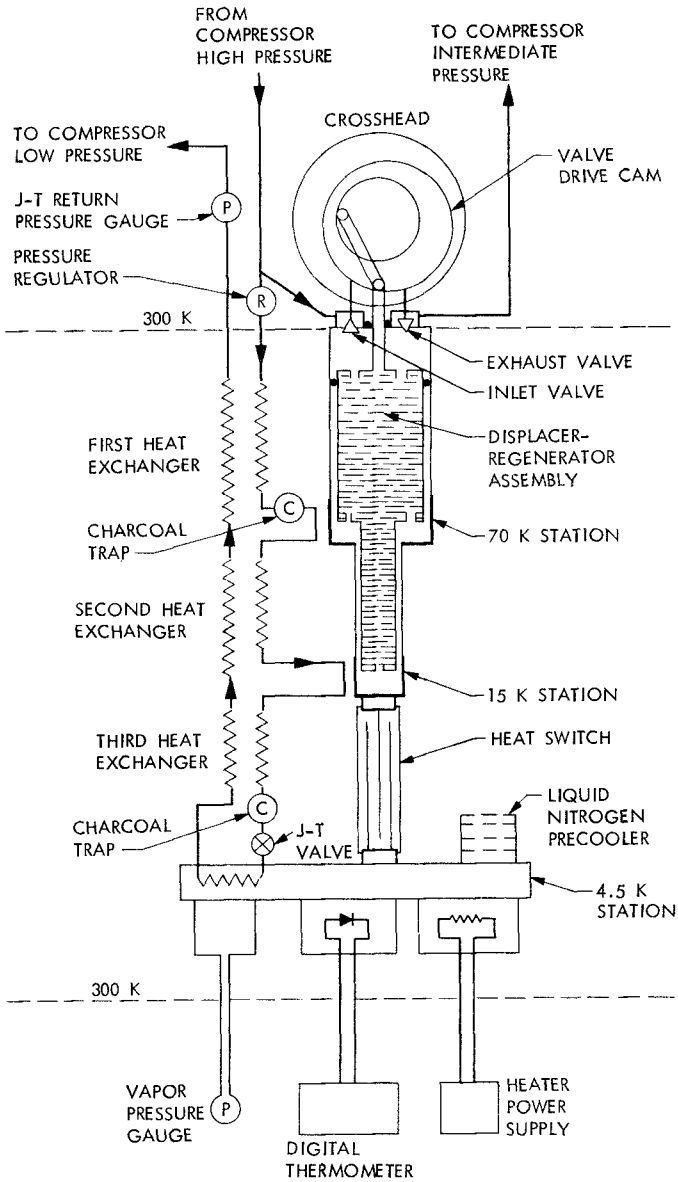


Fig. 1. Schematic diagram for CCR

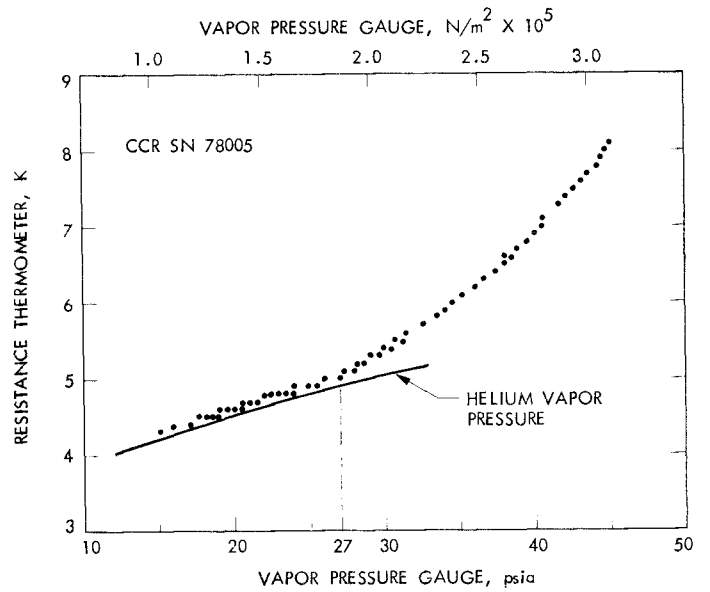


Fig. 2. Comparison of temperature sensing devices

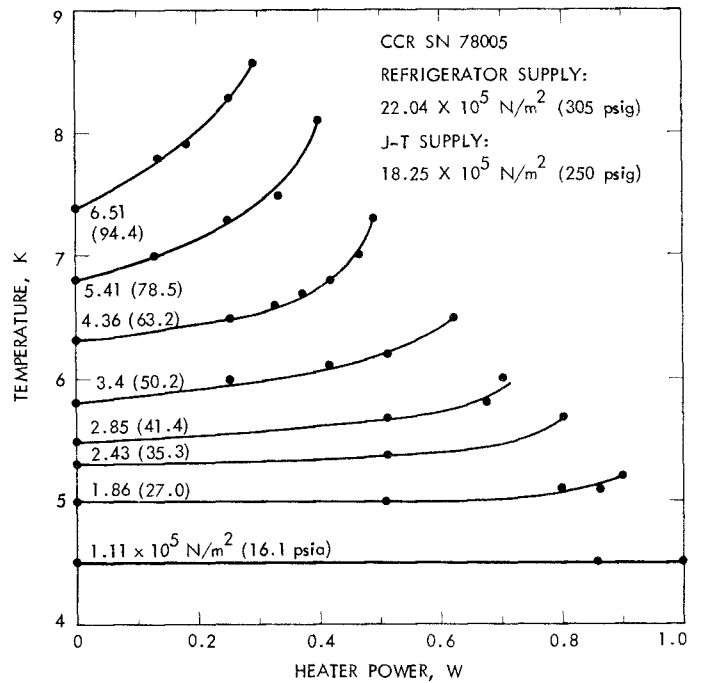


Fig. 3. Temperature as a function of the applied heat load for several J-T return pressures

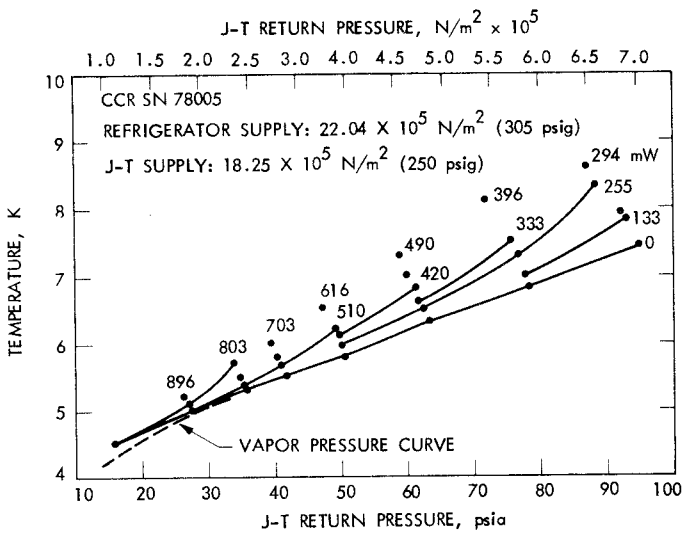


Fig. 4. Measured cooling capacity as a function of J-T return pressure

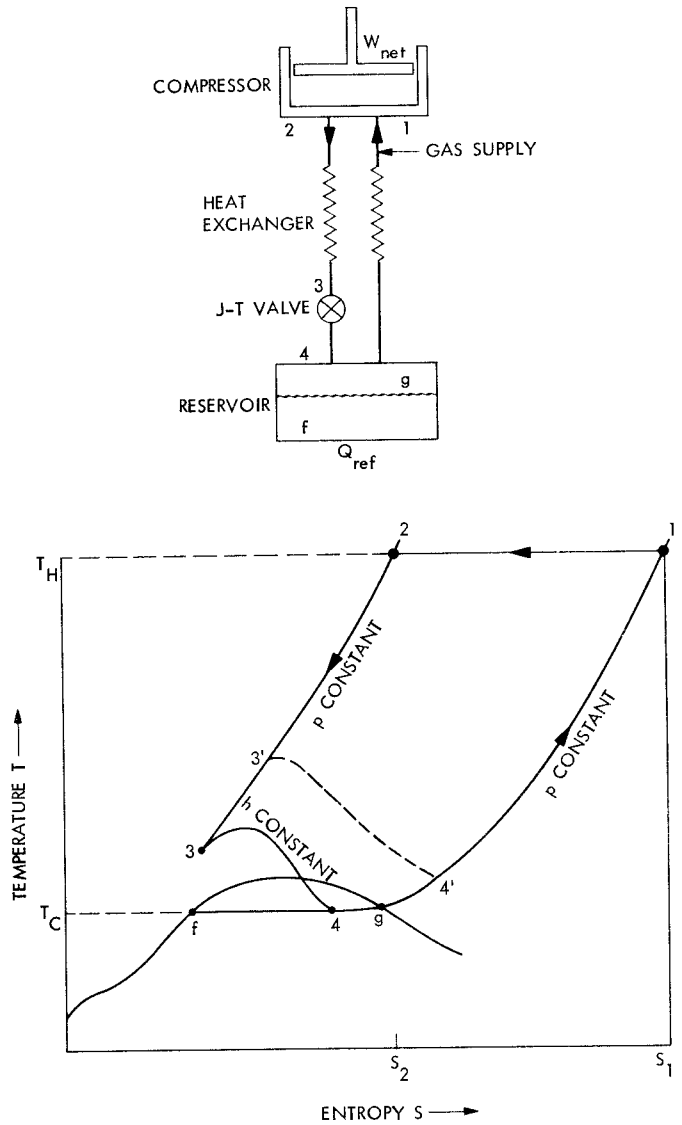


Fig. 5. Thermodynamic cycle and flow diagram for Linde-Hampson refrigerator